Structural vibration reduction optimization by switch shunting of piezoelectric elements

Julien Ducarne, Olivier Thomas, Jean-François Deü

▶ **To cite this version:**

Julien Ducarne, Olivier Thomas, Jean-François Deü. Structural vibration reduction optimization by switch shunting of piezoelectric elements. ASME International Mechanical Engineering Congress and Exposition, IMECE 2007, Nov 2007, Seattle, Washington, United States. pp.797-816, 10.1177/1045389X1036783 . hal-03179543

HAL Id: hal-03179543
https://hal.science/hal-03179543

Submitted on 13 Mar 2024

HAL is a multi-disciplinary open access archive for the deposit and dissemination of scientific research documents, whether they are published or not. The documents may come from teaching and research institutions in France or abroad, or from public or private research centers.

L'archive ouverte pluridisciplinaire **HAL**, est destinée au dépôt et à la diffusion de documents scientifiques de niveau recherche, publiés ou non, émanant des établissements d'enseignement et de recherche français ou étrangers, des laboratoires publics ou privés.

STRUCTURAL VIBRATION REDUCTION OPTIMIZATION BY SWITCH SHUNTING OF PIEZOELECTRIC ELEMENTS

J. Ducarne O. Thomas J.-F. Deü
Structural Mechanics and Coupled Systems Laboratory,
CNAM, 2 rue Conté,
75003 Paris, France
Email: {julien.ducarne,olivier.thomas,deu}@cnam.fr

ABSTRACT

This work deals with the damping of structural vibrations by means of Synchronized Switch Damping (SSD) techniques on piezoelectric elements. Piezoelectric patches are attached to the vibrating structure and connected to an electrical circuit that includes a switch. The latter allows to continuously switch the piezoelectric elements from an open-circuit state to a specific electric impedance, synchronously with the mechanical oscillations. The present study focuses on two goals: (i) the quantification of the added damping (ii) the optimization of the electric circuit parameters.

The free and forced responses of one mode of the mechanical structure are studied in detail. The precise time response of the system is obtained with semi-analytical models for the two cases where the electrical impedance is a simple resistance or a resistance and an inductance. The added damping of the oscillations is estimated analytically. In all cases, it is found that the piezoelectric coupling coefficient has to be maximized in order to maximize the added damping. In the case of SSDI, an optimal value of the electric circuit quality factor is obtained.

1 INTRODUCTION

Structural vibration damping can be achieved by several means. On the one hand, viscoelastic materials are widely used for their ability to dissipate mechanical energy. Piezoelectric materials, on the other hand, convert mechanical energy into electrical energy and conversely. Many different applications of piezoelectric materials take advantage of this property. In active control techniques, a control device is connected to piezoelectric elements bonded on the structure. The latter are used either as actuators for the output or as sensors for the input. In passive shunt techniques, piezoelectric elements are connected to electric circuits (shunts) that dissipate energy and are used simultaneously as sensors and actuators. [1, 2].

This article deals with Synchronized Switch Damping (SSD) techniques, introduced by Guyomar et al. [3, 4] and Clark et al. [5]. An electric circuit including a switch is connected to the piezoelectric elements. The switch is left open most of the time and is closed every time the structure reaches a maximum of amplitude, for a short time long enough to obtain an opposition of the voltage imposed at the piezoelectric elements. The main effect is that the voltage is viewed by the structure as a force that changes of sign at each oscillations and that is thus opposed to its motion. This method has the advantages of being almost passive (as only a small amount of energy is needed to power the switch) and unconditionnaly stable. Because of the synchronization of the electric circuit on the structural oscillations, no precise tuning of the electric parameters on the mechanical frequency characteristics is needed.

The first goal of this article is to built an efficient reduced order electro-mechanical model that is able to catch all the main behaviors observed experimentally and that will be used to design the switch device and to understand its behavior. In particular, the mechanisms that govern the energy dissipation are not fully understood at the moment, mostly because the switch opening and closing operations bring non-smooth time responses, whose non-linear nature lead to transfers of energy between vibration

modes. As a consequence, a multi degree-of-freedom (dof) electromechanical model is essential.

In a first part, a general electro-mechanical model of a cantilever beam with piezoelectric elements coupled to an electric circuit is presented. A modal approach is used to derive the discretized equations of motion, obtained by expanding the unknown displacement of the beam onto the basis of vibration modes of the structure with piezoelectric elements short circuited. An additional equation is added to take into account the electric dof

Then, some results about the optimization of the electric parameters of the switch as well as the estimation of the added damping are obtained by reducing the model to one mechanical dof and one electrical dof, in both cases where the electrical circuit is a simple resistance (SSDS, Synchronized Switch Damping on Short) or a resistance and an inductance (SSDI, Synchronized Switch Damping on Inductor). The free time response of the system is precisely simulated by considering successively all switch operations with recurrence analytical relations. The forced response is obtained in a similar way, for excitation at resonance and out of resonance.

2 ELECTROMECHANICAL MODEL OF A BEAM WITH PIEZOELECTRIC ELEMENTS

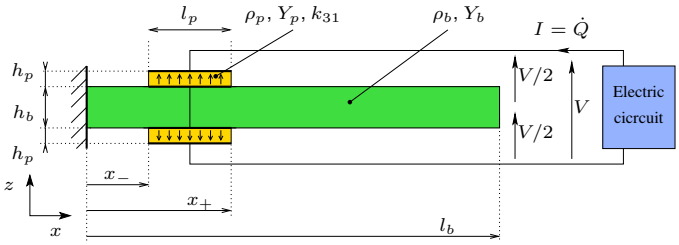

Figure 1. Structure with piezoelectric elements coupled to an electric circuit

A cantilever beam, already used in [2], is partially covered with two collocated piezoelectric elements, polarized in opposite directions. The electrodes are connected in series to the switched shunt. We use the "31" coupling of the piezoelectric elements that couples longitudinal (x direction) deformations with the electric field in the transverse (z direction), normal to the electrodes (Fig. 1). As the polarization directions are opposite in the elements, only the flexion movements of the beam are coupled to the electric circuit.

The beam with the piezoelectric elements is modeled with Euler-Bernoulli assumptions so that it is equivalent to an homogeneous beam with material properties piecewise constant as a function of x. The beam material is elastic, homogeneous and isotropic. The piezoelectric material law is reduced to the x direction for the mechanical part (stress σ_1 and strain ε_1) and to the z direction for the electric part (electric displacement D_3 and electric field E_3):

$$\begin{cases} \sigma_1 = C_{11}^* \varepsilon_1 - e_{31}^* E_3, \\ D_3 = e_{31}^* \varepsilon_1 + \epsilon_{33}^* E_3, \end{cases}$$

Where C_{11}^*, ϵ_{33}^* and e_{31}^* are the modified elastic, dielectric and piezoelectric constants due to Euler-Bernoulli assumptions.

The electric field in the piezoelectric elements is supposed constant in the transverse z direction as well as in the longitudinal x direction. The free charge on the electrodes is obtained by integrating the electric displacement flux across the electrodes. The dimensionless equation of motion for the transverse displacement $w(x,t)$ at a point x of the beam and the electric equation for the free charge $Q(t)$ in one of the electrodes and the electric potential $V(t)$ in the shunt (Fig. 1), at time t, write:

$$m\frac{\partial^2 w}{\partial t^2} + \frac{\partial^2}{\partial x^2}\left(D\frac{\partial^2 w}{\partial x^2}\right) + \alpha^2 \Delta\left[\frac{\partial w}{\partial x}\right]_{x=x_-}^{x=x_+} = \alpha \Delta\, Q + p \tag{1}$$

$$Q = \alpha\left[\frac{\partial w}{\partial x}\right]_{x_-}^{x_+} + V, \tag{2}$$

with

$$\Delta(x) = \frac{\partial}{\partial x}[\delta(x - x_-) - \delta(x - x_+)], \tag{3}$$

where $\delta(x)$ denotes the Dirac function. In the above equations, m and D denote the mass by unit length and the flexural stiffness, piecewise constant due to the presence of the piezoelectric elements. p is an external transverse force by unit length. α denotes a dimensionless parameter that represents the electromechanical coupling.

The piezoelectric elements effects appears by (i) two opposite concentrated bending moments (Eq. (3)) applied at the ends x_- and x_+ of the piezoelectric elements, in opposite directions and proportional to voltage $V(t)$ (eliminate Q between Eqs. (1) and (2)); (ii) a free electric charge $Q(t)$ proportional to the slope difference at the ends x_- and x_+ of the piezo elements; (iii) additives mass and flexural stiffness.

A solution to partial differential equations (1) and (2) is obtained by expanding $w(x,t)$ onto the eigenmode basis of the

short-circuited beam $(\Phi_r(x), \omega_r)$, solutions of :

$$\frac{\partial^2}{\partial x^2}\left(D\frac{\partial^2 \Phi_r}{\partial x^2}\right) - m\omega_r^2 \Phi_r = 0. \tag{4}$$

The problem then writes:

$$w(x,t) = \sum_{r=1}^{+\infty} \Phi_r(x) q_r(t). \tag{5}$$

$$\begin{cases} \ddot{q}_r + 2\xi_r\omega_r\dot{q}_r + \omega_r^2 q_r + \omega_r k_r \sum_{i=1}^{+\infty} \omega_i k_i q_i - \omega_r k_r Q = \tilde{F}_r \\ Q - \sum_{i=1}^{+\infty} \omega_i k_i q_i = V. \end{cases} \tag{6}$$

where $\Phi_r(x)$, ω_r, ξ_r, k_r and $\tilde{F}_r$ denote respectively the mode shape, angular frequency, the mechanical damping factor, the modal coupling coefficient and the modal forcing of the r-th mode in short circuit. Coupling coefficient k_r, whose role will be emphasized later, depends of the material parameters (the beam and piezoelectric material Young moduli Y_b and Y_p, piezoelectric constant k_{31}), the dimensions (lengths l_b, l_p; thicknesses h_b, h_p) and mode natural frequency and shape. It writes:

$$k_r = \sqrt{6}\, k_{31} \sqrt{\frac{Y_p}{Y_b}} \sqrt{\frac{l_b}{l_p}} \left(1 + \frac{h_p}{h_b}\right) \sqrt{\frac{h_p}{h_b}} \frac{1}{\omega_r} \left[\frac{\partial \Phi_r}{\partial x}\right]_{x=x_-}^{x=x+}. \tag{7}$$

The initial set of partial differential equations (1) is replaced by an infinite set of coupled ordinary differential equations, each one corresponding to a mechanical mode and one additional for the electric part.

When the circuit is open ($\dot{Q} \equiv 0$ in Eq. (6)), the modes are coupled with one another by terms $\omega_r k_r \omega_i k_i$ that can be viewed as an *added stiffness* as compared to the short-circuit condition ($V \equiv 0$). The angular frequencies $\hat{\omega}_r$ in open circuit condition can be obtained by diagonalisation of Eqs. (6) truncated to N modes, with $Q \equiv 0$. However, when the eigenfrequencies are far apart, a good estimation of k_r can be obtained by reducing Eqs. (6) to a single degree-of-freedom (dof). One can then show that modal coupling coefficient k_r is very close to the effective coupling coefficient k_{eff} [6]:

$$k_r \simeq k_{\text{eff}} = \sqrt{\frac{\hat{\omega}_r^2 - \omega_r^2}{\omega_r^2}}. \tag{8}$$

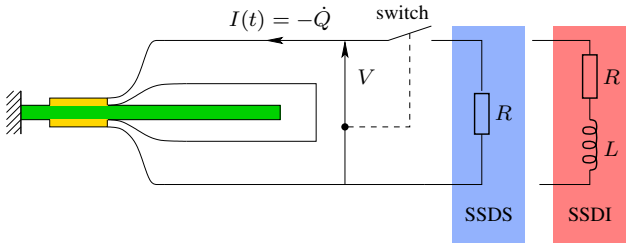

Figure 2. Structure with switched shunts

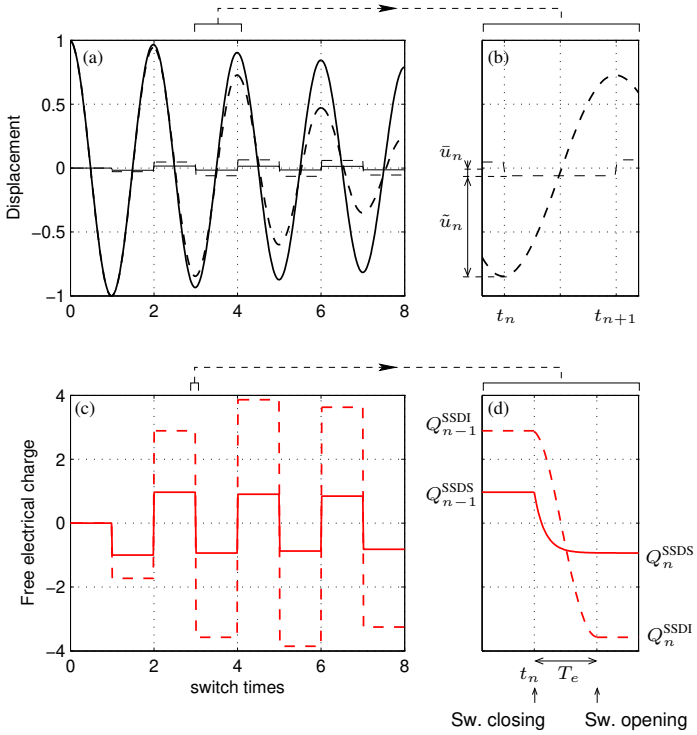

Figure 3. Time evolution of displacement $u(t)$ (a) and free electric charge $Q(t)$ (c), in SSDS (solid line) and SSDI (dotted line) case, with zoom on one mechanical evolution step (b) and one electrical evolution step (d)

3 FREE RESPONSE WITH SSD: A ONE DOF MODEL

In this section, the free response of the beam connected to a SSD electric circuit and around the r-th resonance is investigated. Eqs. (6) are *reduced to a one dof system* by keeping the r-th mode only. We study both cases of Synchronised Switch Damping on Short (SSDS), where the switch is connected to an electrical resistance only and Synchronized Switch Damping on Inductance (SSDI) where the switch is connected to an inductance and a resistance. One obtains the following equations, where $u(t) \equiv q_r(t)$ denotes the only remaining modal coordi-

nate:

$$\text{Mechanical part:} \quad \ddot{u} + \hat{\omega}_r^2 u - k_r \omega_r Q = 0, \quad (9a)$$

$$\text{Switch open:} \quad \dot{Q} = 0, \quad (9b)$$

$$\text{SSDS closed:} \quad \tau_e \dot{Q} + Q - k_r \omega_r u = 0, \quad (9c)$$

$$\text{SSDI closed:} \quad \frac{1}{\omega_e^2}\ddot{Q} + \frac{2\xi_e}{\omega_e}\dot{Q} + Q - k_r \omega_r u = 0. \quad (9d)$$

In the above equations, τ_e stands for the time constant of the SSDS shunt, linked to resistance R. ξ_e and ω_e denotes the damping factor (linked to resistance R) and the angular frequency (linked to inductance L) of the SSDI shunt.

The switch command strategy is now explained. Most of the time, the switch is open : no current flows ($\dot{Q} = 0$) and the free electric charge Q on the piezoelectric elements is constant (Eq. (9b)). In this case, the beam is free to oscillate at the open circuit angular frequency $\hat{\omega}_r = \omega_r\sqrt{1+k_r^2}$ (Eq. (9a)). Every time the piezo voltage reaches a maximum, the switch is closed for a brief time T_e, very small compared to the mechanical period of the structure. In the case of SSDS, this time is sufficient for the charge to reach an equilibrium. In the case of SSDI, this time is precisely chosen as half a period of the equivalent RLC electrical circuit (the piezoelectric elements are equivalent to a capacitance C, in series with the resistance R and the inductance L). In both cases, the effect of the electric charge on the mechanical structure is to create a constant force that changes of sign synchronously with the oscillations and that opposes itself to the motion, almost like a dry damper.

3.1 SSDS model

To investigate the behavior of the system, the following assumptions are used, illustrated by Fig. 3. The switch is closed every half-period of the mechanical oscillations, at time $t_n = n\pi/\hat{\omega}_r$ (fig. 3(a,c)). The closed switch state lasts T_e, assumed short compared to the time evolution of the mechanical part of the system: $T_e \ll \pi/\hat{\omega}_r$ (fig. 3(d)). After $t_n + T_e$, the free electric charge reaches an equilibrium value of Q_n ; between t_n and t_{n+1}, $u(t)$ is therefore solution of Eq. (9a):

$$\ddot{u} + \hat{\omega}_r^2 u - k_r \omega_r Q_n = 0, \quad (10)$$

that writes:

$$u(t)|_{t_n<t<t_{n+1}} = \bar{u}_n + \tilde{u}_n \cos(\hat{\omega}_r(t-t_n)), \quad (11)$$

with constant part $\bar{u}_n$ depending of the free charge :

$$\bar{u}_n = \frac{k_r \omega_r}{\hat{\omega}_r^2} Q_n. \quad (12)$$

The continuity of u during the switch at t_{n+1} gives the value of the oscillating parts $\tilde{u}_n$:

$$u(t_{n+1}) = \bar{u}_n - \tilde{u}_n = u(t_{n+1}+T_e) = \bar{u}_{n+1} + \tilde{u}_{n+1}. \quad (13)$$

In the case of SSDS, the electric part behaves as a first order system (Eq. (9c)):

$$\tau_e \dot{Q} + Q - k_r \omega_r u(t_{n+1}) = 0, \quad Q(t_{n+1}^-) = Q_n. \quad (14)$$

As $\tau_e \simeq T_e \ll \pi/\hat{\omega}_r$,, the mechanical part $u(t)$ is considered constant during the closed switch state. At $t_{n+1} + T_e$, the charge has reached the equilibrium and the final value is $Q_{n+1} = k_r\omega_r u(t_{n+1}) = k_r\omega_r(\bar{u}_n - \tilde{u}_n)$. With Eq. (12), one obtains:

$$\bar{u}_{n+1} = \frac{k_r^2 \omega_r^2}{\hat{\omega}_r^2}(\bar{u}_n - \tilde{u}_n). \quad (15)$$

3.2 SSDI model

In the case of SSDI, the mechanical part can also be modeled with Eqs. (12) and (13). The electrical part when the switch is closed behaves as a damped harmonic oscillator (Eq. (9d)) while the mechanical part $u(t)$ remains constant :

$$\frac{1}{\omega_e^2}\ddot{Q} + \frac{2\xi_e}{\omega_e}\dot{Q} + Q - k_r\omega_r u(t_{n+1}) = 0, \quad Q(t_{n+1}) = Q_n \quad (16)$$

The switch remains closed for half a period of the damped harmonic oscillator : $T_e = \pi/(\omega_e\sqrt{1-\xi_e^2})$; The final value of the free electric charge is attained at the first overshoot of the electrical oscillations :

$$\begin{aligned} Q_{n+1} &= Q(t_{n+1}+T_e) \\ &= k_r\omega_r(\bar{u}_n - \tilde{u}_n) - X\left[Q_n - k_r\omega_r(\bar{u}_n - \tilde{u}_n)\right], \end{aligned}$$

with the overshoot factor defined by:

$$X = \exp\left(\frac{-\pi\xi_e}{1-\xi_e^2}\right), \quad (17)$$

that depends only on ξ_e. Taking (12) into account, one obtains

$$\bar{u}_{n+1} = (1-X)\frac{k_r^2}{1+k_r^2}(\bar{u}_n - \tilde{u}_n) - X\bar{u}_n \quad (18)$$

3.3 Decay rate

The values of $(\bar{u}_n)_{n\in\mathbb{N}}$ and $(\tilde{u}_n)_{n\in\mathbb{N}}$ can be written with a recurrence relationship by taking into account Eqs. (12), (13) and (15) or (18). For both cases of SSDS and SSDI :

$$\mathbf{u}_n = \mathbf{A}\mathbf{u}_{n-1} = \mathbf{A}^n\mathbf{u}_0, \tag{19}$$

with $\mathbf{u}_n = (\tilde{u}_n\ \bar{u}_n)^{\mathrm{t}}$ and the transfer matrix $\mathbf{A}$ depending of the electrical parameters :

$$\mathbf{A}^{\text{SSDS}} = \frac{1}{1+k_r^2}\begin{pmatrix} -1 & 1 \\ -k_r^2 & k_r^2 \end{pmatrix}, \tag{20}$$

$$\mathbf{A}^{\text{SSDI}} = \frac{1}{1+k_r^2}\begin{pmatrix} Xk_r^2-1 & 1+X \\ -k_r^2(1+X) & k_r^2-X \end{pmatrix}. \tag{21}$$

With Eq. (19), $(\bar{u}_n)_{n\in\mathbb{N}}$, $(\tilde{u}_n)_{n\in\mathbb{N}}$ can be written as a sum of two geometric sequences :

$$\begin{cases} \bar{u}_n = \bar{a}_1\lambda_1^n + \bar{a}_2\lambda_2^n \\ \tilde{u}_n = \tilde{a}_1\lambda_1^n + \tilde{a}_2\lambda_2^n \end{cases}, \tag{22}$$

where λ_1 and λ_2 are the eigenvalues of $\mathbf{A}$. If $|\lambda_1| \geq |\lambda_2|$, one can show with Eqs. (11) and (22) that:

$$\begin{aligned} |u(t_n)| &\leq |\bar{u}_n| + |\tilde{u}_n| \\ &\leq (|\bar{a}_1| + |\tilde{a}_1| + (|\bar{a}_2| + |\tilde{a}_2|)\frac{|\lambda_2|^n}{|\lambda_1|^n})|\lambda_1|^n \\ &\leq a|\lambda_1|^n. \end{aligned}$$

with $a = |\bar{a}_1| + |\tilde{a}_1| + |\bar{a}_2| + |\tilde{a}_2|$. The above inequalities show that $u(t)$ is bounded by a decaying exponential function of decay rate μ, defined by :

$$ae^{-\mu t_n} = a|\lambda_1|^n, \tag{23}$$

where

$$\mu = -\frac{\hat{\omega}_r}{\pi}\ln(|\lambda_1|). \tag{24}$$

μ is positive when $|\lambda_1| < 1$ and it increases when $|\lambda_1|$ decreases. As a consequence, *one has to minimize the modulus of the eigenvalue $|\lambda_1|$ of $\mathbf{A}$ of greatest modulus in order to increase the decay rate of the free response of the structure, and thus to increase damping*. As the time evolution frequency of $u(t)$ is very close to $\hat{\omega}_r$, it is convenient to define *the damping factor ξ of the free response of the structure with SSD* by:

$$\mu = \xi_{\text{tot}}^{\text{SSD}}\hat{\omega}_r \quad \Longrightarrow \quad \xi_{\text{tot}}^{\text{SSD}} = -\frac{\ln(|\lambda_1|)}{\pi}. \tag{25}$$

3.4 Optimization of SSDS

In the case of SSDS, Eq. (20) leads to obtain

$$|\lambda_1| = \frac{1-k_r^2}{1+k_r^2}, \quad \lambda_2 = 0.$$

The damping factor is then (Eq. (25)):

$$\xi_{\text{tot}}^{\text{SSDS}} = -\frac{1}{\pi}\ln\left(\frac{1-k_r^2}{1+k_r^2}\right). \tag{26}$$

The damping factor does not depend on τ_e and thus on the electric resistance. One has just to ensure that the resistance is small enough so that the electric time evolution is much smaller than the mechanical period of the system. In order to increase $\xi_{\text{tot}}^{\text{SSD}}$, one has to increase k_r only. This can be done by optimizing the piezoelectric elements associated to the structure, using (7).

3.5 Optimization of SSDI

In the case of SSDI, λ_1 and λ_2 depend on ξ_e, the damping factor of the electric circuit. Figure 4 shows the eigenvalues moduli $|\lambda_1|$ and $|\lambda_2|$ as a function of ξ_e. One can observe that the eigenvalues are complex conjugates for low values of ξ_e and distinct real for high values of ξ_e. An optimal value ξ_e^{opt} of ξ_e is obtained if the modulus of the eigenvalue of greatest modulus is minimum. This is the case if (Eq. (21))

$$|\lambda_1| = |\lambda_2| = \frac{1-k_r}{1+k_r}, \tag{27}$$

which lead to the optimal value of ξ_e:

$$X^{\text{opt}} = \frac{(1-k_r)^2}{(1+k_r)^2}, \quad \xi_e^{\text{opt}} = \sqrt{\frac{\ln(X^{\text{opt}})^2}{\ln(X^{\text{opt}})^2+\pi^2}}, \tag{28}$$

The total damping factor of the free response of the structure with SSDI is then:

$$\xi_{\text{tot}}^{\text{SSDI}} = -\frac{1}{\pi}\ln\left(\frac{1-k_r}{1+k_r}\right). \tag{29}$$

Figure 4 shows the evolution of ξ_e^{opt} as a function of k_r.

Figure 5 show the time evolution of $u(t)$ for three different values of ξ_e and confirms the above results. For $\xi_e < \xi_e^{\text{opt}}$ a beating phenomenon appears ; for $\xi_e > \xi_e^{\text{opt}}$, the greatest eigenvalue modulus increases and the decay is slower ; the optimal value of ξ_e ensures the greatest decay rate.

In order to fully optimize the system, we have to first maximize k_r in (29) by optimizing the piezoelectric elements using (7), and then to choose the appropriate ξ_e. The result will only depend of k_r. One can note that ω_e, directly linked to inductance L, has no influence on the system behavior: one has just to chose ω_e as high as possible to ensure that the electric period is much smaller than the mechanical period.

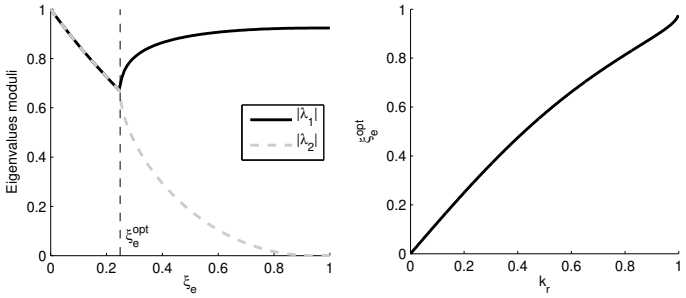

Figure 4. (left) Moduli of eigenvalues of $\mathbf{A}^{\text{SSDI}}$ for $k_r = 0.2$. (right) Optimal electrical damping ξ_e^{opt} as function of k_r

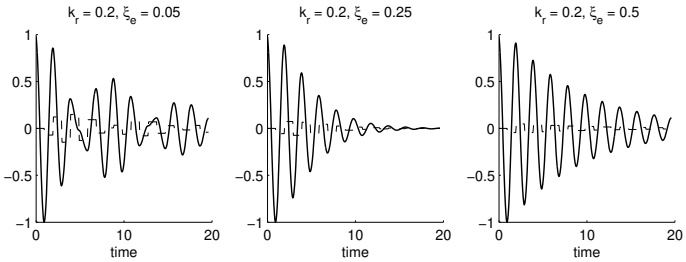

Figure 5. Time evolution of displacement $u(t)$ (solid line) and $\bar{u}_n$ (dotted) with SSDI, for three values of ξ_e. (left): low ξ_e; (center): optimal ξ_e; (right) high ξ_e.

3.6 Effect of mechanical damping

The previous results have been obtained by neglecting the mechanical damping ξ_r. To take it into account, Eq. (10) is replaced by

$$\ddot{u} + 2\xi_r\omega_r\dot{u} + \hat{\omega}_r^2 u - k_r\omega_r Q_n = 0, \tag{30}$$

whose solution is

$$u(t)|_{t_n<t<t_{n+1}} = \bar{u}_n + \tilde{u}_n e^{-\xi_r\hat{\omega}_r}\cos(\tilde{\omega}_r(t-t_n)), \tag{31}$$

with $\tilde{\omega}_r = \hat{\omega}_r\sqrt{1-\xi_r^2}$. The value of u just before a switch is now

$$u(t_{n+1}) = \bar{u}_n - X_r\tilde{u}_n, \tag{32}$$

where $X_r = \exp[-\pi\xi_r/(1-\xi_r^2)]$ is the overshoot factor of the mechanical oscillator. Relationship (19) can be rewritten to take into account the mechanical damping :

$$\mathbf{u}_n = \mathbf{AB}\mathbf{u}_{n-1} = (\mathbf{AB})^n\mathbf{u}_0, \quad \mathbf{B} = \begin{pmatrix} X_r & 0 \\ 0 & 1 \end{pmatrix}. \tag{33}$$

where matrix $\mathbf{B}$ represents the mechanical losses. With analogous arguments than those of sections 3.4 and 3.5, we can obtain the eigenvalues λ_1 and λ_2 of matrix $\mathbf{AB}$ and get the following results.

In the case of SSDS we obtain $|\lambda_1| = (X_r - k_r^2)/(1+k_r^2)$ and $\lambda_2 = 0$. The damping ratio of the free response then writes:

$$\xi_{\text{tot}}^{\text{SSDS}} = -\frac{\sqrt{1+k_r^2}}{\pi}\ln\left(\frac{X_r - k_r^2}{1+k_r^2}\right). \tag{34}$$

For the SSDI system, the optimal value of ξ_e depends of k_r and ξ_r, with a complicated analytical expression. However, the optimal value ξ_e^{opt} with mechanical damping ($\xi_r \neq 0$) is found very close the optimal value obtained without damping (Eq. 28) added to the mechanical damping ξ_r (Fig. 6):

$$\xi_e^{\text{opt}}|_{\xi_r\neq 0} \simeq \xi_e^{\text{opt}}|_{\xi_r=0} + \xi_r. \tag{35}$$

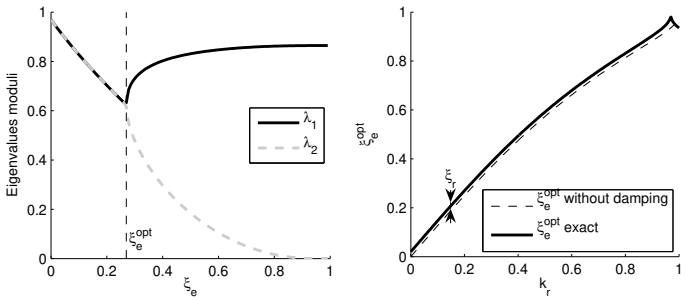

Figure 6. (left) Moduli of eigenvalues of $\mathbf{A}^{\text{SSDI}}\mathbf{B}$ for $k_r = 0.2$ and $\xi_r = 2\%$; (right) optimal electrical damping ξ_e^{opt} as functions of k_r whith mechanical damping

In both cases of SSDS and SSDI, we can define the added damping $\xi_{\text{add}} = \xi_{\text{tot}} - \xi_r$. Figure 7 shows that ξ_{add} is almost independant of the mechanical damping ξ_r. It means that *a good estimation of the damping ratio of the free response of the structure*

with switch can be obtained by adding the mechanical damping ratio ξ_r to the values of ξ of Eqs. (26) and (29) (obtained with $\xi_r = 0$):

$$\xi_{\text{tot}}^{\text{SSDS}} \simeq \xi_{\text{tot}}^{\text{SSDS}}\big|_{\xi_r=0} + \xi_r, \quad \xi_{\text{tot}}^{\text{SSDI}} \simeq \xi_{\text{tot}}^{\text{SSDI}}\big|_{\xi_r=0} + \xi_r. \quad (36)$$

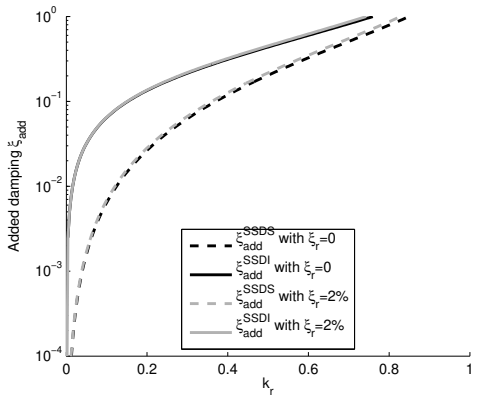

Figure 7. Added damping as a function of k_r with and without mechanical damping

4 FORCED RESPONSE WITH SSD: A 1 DOF MODEL

4.1 Time response of the system

We study the beam with SSDS or SSDI in forced oscillations around the r-th mode. Like in section 3, Eqs. (6) are reduced to a one dof system by keeping the r-th mode only. The modal forcing is written $\tilde{F}_r(t) = F_r \cos \Omega t$ and the problem is defined by Eqs. (9b-d) with Eq. (9a) replaced by:

$$\ddot{u} + 2\xi_r \hat{\omega}_r \dot{u} + \hat{\omega}_r^2 u - k_r \omega_r Q_n = F_r \cos(\Omega t). \quad (37)$$

The switch strategy is exactly the same than the one described in section 3. Between t_n and t_{n+1}, the switch is opened and the solution of Eq. (37) is written:

$$u(t)_{t_n<t<t_{n+1}} = \bar{u}_n + u_T(t) + u_F(t), \quad (38)$$

where $\bar{u}_n$, $u_T(t)$ and $u_F(t)$ are respectively the stationary, transient and forced solution of Eq. (37). $\bar{u}_n$ is the stationary response of the system to the free electric charge Q_n applied; like in Eq. (10), it writes:

$$\bar{u}_n = \frac{k_r \omega_r}{\hat{\omega}_r^2} Q_n.$$

$u_T(t)$ can be written:

$$u_T(t) = e^{-\xi_r \hat{\omega}_r \hat{t}} \left[\tilde{u}_n \cos(\tilde{\omega}_r \hat{t}) + \tilde{u}'_n \sin(\tilde{\omega}_r \hat{t}) \right], \quad (39)$$

with $\tilde{\omega} = \hat{\omega}_r \sqrt{1-\xi_r^2}$ and $\hat{t} = t - t_n$. $\tilde{u}_n$ and $\tilde{u}'_n$ are two coefficients, that depend on the initial conditions right after the n-th switch. $u_F(t)$ can be written:

$$u_F(t) = \frac{\hat{\omega}_r^2 - \Omega^2}{d(\Omega)} \cos \Omega t - \frac{2\xi_r \omega_r \Omega}{d(\Omega)} \sin \Omega t, \quad (40)$$

with $d(\Omega) = (\hat{\omega}_r^2 - \Omega^2)^2 + 4\xi_r^2 \omega_r^2 \Omega^2$.

The values of $(t_n, Q_n, \bar{u}_n, \tilde{u}_n, \tilde{u}'_n)_{n\in\mathbb{N}}$ are obtained with the same arguments than in sections 3.1 and 3.2, and depends on the value of t_n. t_n is the first time after t_{n-1} where $u(t)$ reaches a maximum, e.g. when $\dot{u}(t) = 0$. As $u(t)$, for $t > t_{n-1}$, is the sum of a constant, a harmonic and an exponentially decaying oscillating part (Eq. (38)), there is no analytical expression for t_n, and neither for Q_n, $\bar{u}_n$, $\tilde{u}_n$ and $\tilde{u}'_n$. The values of Q_n, $\bar{u}_n$, $\tilde{u}_n$ and $\tilde{u}'_n$ are computed knowing their values at step $n-1$. Then, t_{n+1} is obtained by computing numerically the first zero of $\dot{u}(t)$, with Eqs. (38-40). The system whole time response is then obtained by concatenating the solutions obtained at each step (between two switch operations).

4.2 Response with SSDS

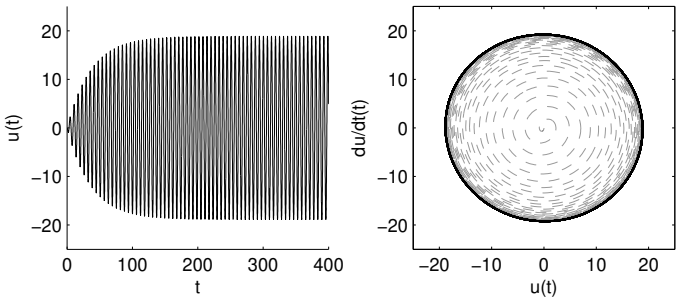

Figure 8. Time evolution of mechanical displacement $u(t)$ with SSDS and phase space, for $k_r = 0.2$ and $\xi_r = 0.1\%$; system forced near resonance ($\Omega \simeq \omega_r$)

The displacement time evolution with SSDS is found to be always converging towards a steady state response (Fig. 8) that is periodic of angular frequency Ω (the excitation frequency). In order to evaluate the response of the system as a function of excitation frequency Ω, the root mean square (RMS) value u^{RMS}

of the time evolution of $u(t)$ is numerically evaluated and plotted as a function of forcing frequency Ω, for various Ω around resonance $\hat{\omega}_r$. u^{RMS} is defined by:

$$u^{\text{RMS}} = \sqrt{\frac{1}{T}\int_0^T u^2(t)\,dt}, \tag{41}$$

and computed with T sufficiently large so that the steady state is attained. Figure 9 is obtained. It is similar to a frequency response function plot, but it takes into account all the spectral components of $u(t)$.

The maximum amplitude is obtained at resonance. To evaluate the efficiency of the system, the attenuation $A_{\text{dB}}^{\text{SSDS}}$ is defined as the difference, in dB, between the peak amplitude of the system with SSDS and the amplitude at resonance of the system in short circuit (fig. 9). $A_{\text{dB}}^{\text{SSDS}}$ depends only on k_r and ξ_r and is plotted on Fig. 9. It is found that k_r has to be as high as possible in order to maximize the attenuation brought by the switch.

Finally, as in the case of the free response (section 3.4), no optimal value of the electric resistance is obtained: one has just to ensure that R is small enough so that the electric time constant is much lower that the mechanical period of the system.

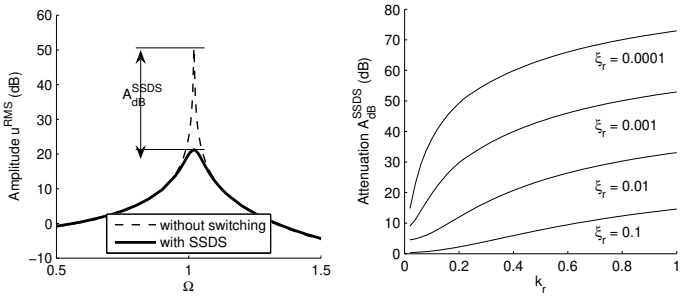

Figure 9. (left) RMS value u^{RMS} of time response $u(t)$ as a function of excitation frequency Ω, for $k_r = 0.2$ and $\xi_r = 0.1\%$. (right) $A_{\text{dB}}^{\text{SSDS}}$ as a function of k_r, for different mechanical damping factors ξ_r

4.3 Response with SSDI

When observing the time response of the system with SSDI, we observed that for low values of ξ_e, the time evolution of the system does not stabilize itself in a periodic steady state signal. An example is given on Fig. 10 (left), where the trajectory in the phase space tends to prove that the system response is chaotic. For higher values of ξ_e, the system response stabilizes itself in a periodic regime of frequency Ω, after a short transient (Fig. 10 (mid, right)).

In a similar way than in the case of SSDS (section 4.2), we can plot the RMS value u^{RMS} of $u(t)$ as a function of excitation frequency Ω and define the attenuation $A_{\text{dB}}^{\text{SSDI}}$ (Fig. 11). Then, the evolution of $A_{\text{dB}}^{\text{SSDI}}$ as a function of ξ_e can be obtained, as shown on Fig. 11 (right). One can observe that above a critical value of ξ_e, the system response is stable and periodic and that $A_{\text{dB}}^{\text{SSDI}}$ decreases when ξ_e increases. This critical value can be chosen as an optimal value ξ_e^{opt} for ξ_e.

Figure 12 (left) shows the evolution of ξ_e^{opt} as a function of k_r, for various values of ξ_r. We find ξ_e^{opt} to be mostly dependent on k_r. Finally, the attenuation $A_{\text{dB}}^{\text{SSDI}}$ obtained with optimal electric damping ($\xi_e = \xi_e^{\text{opt}}$) as a function of k_r for various values of ξ_r is shown on Figure 12(right). Once again, k_r has to be maximized in order to obtain the best possible performance.

As in the case of the free response (section 3.5), no optimal value of the electric inductance L is obtained: one has just to ensure that L is low enough so that the electric time constant is much lower that the mechanical period of the system.

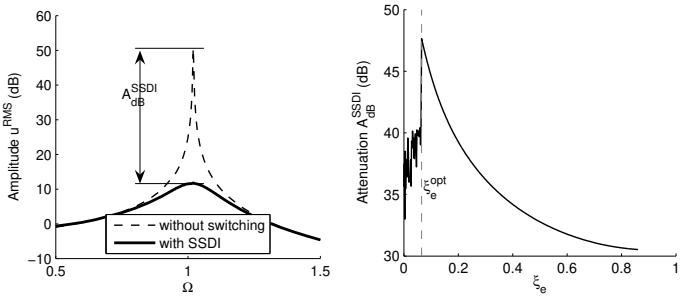

Figure 11. (left) RMS value u^{RMS} of time response $u(t)$ as a function of excitation frequency Ω. (right) Attenuation $A_{\text{dB}}^{\text{SSDI}}$ as a function of ξ_e. In both cases, $k_r = 0.2$ and $\xi_r = 0.1\%$

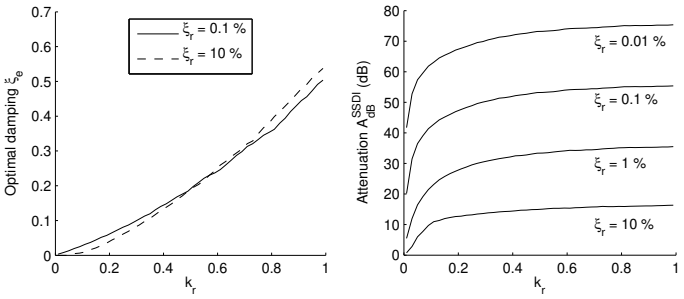

Figure 12. (left) ξ_e^{opt} as a function of k_r; (right) $A_{\text{dB}}^{\text{SSDI}}$ as a function of k_r, for different mechanical damping factors ξ_r

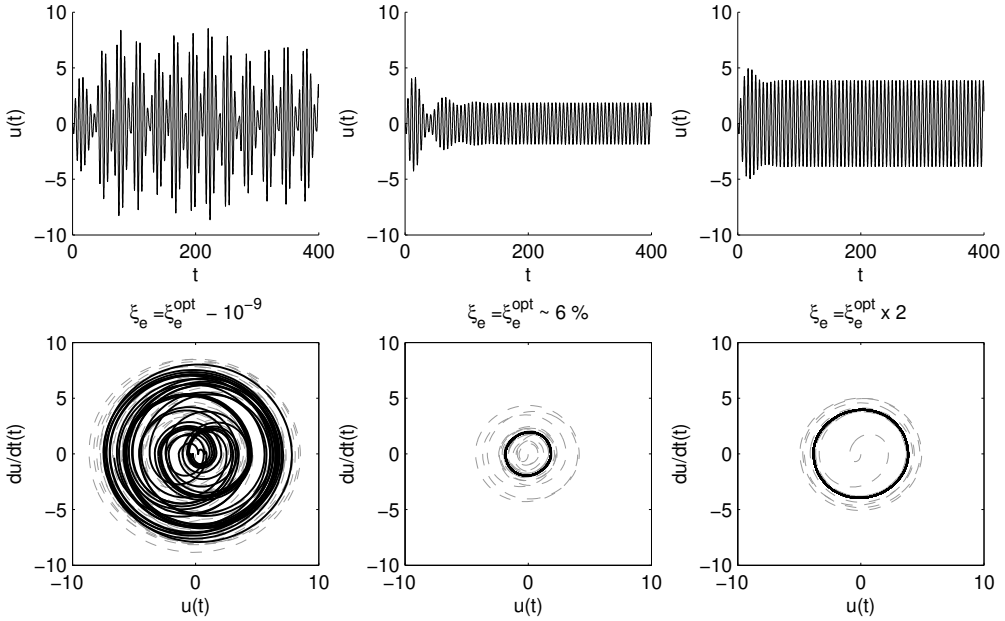

Figure 10. Time evolution of mechanical displacement $u(t)$ with SSDI and phase spaces, for $k_r = 0.2$ and $\xi_r = 0.1\%$. (left): System forced near resonance ($\Omega \simeq \hat{\omega}_r$) with overcritical damping ξ_e; (center) optimal damping ξ_e; (right) large damping ξ_e.

Table 1. Summary of the main characteristics of SSDS and SSDI systems in free and forced response. Numerical values of ξ_{add} and A_{dB} are obtained with $k_r = 0.2, \xi_r = 0.1\%$.

	Free response	Forced response
SSDS	$\xi_{\text{add}} = -\frac{1}{\pi} \ln\left(\frac{1-k_r^2}{k_r^2+1}\right)$	$A_{\text{dB}} = f(k_r, \xi_r)$
	$\xi_{\text{add}} = 2.5\%$	$A_{\text{dB}} = 30$ dB
SSDI	$\xi_{\text{add}} = -\frac{1}{\pi} \ln\left(\frac{1-k_r}{1+k_r}\right)$	$A_{\text{dB}} = f(k_r, \xi_r)$
	$\xi_e^{\text{opt}} = f(k_r)$	$\xi_e^{\text{opt}} = f(k_r)$
	$\xi_{\text{add}} = 10\%$	$A_{\text{dB}} = 46$ dB

5 CONCLUSION

In this article, a multi degree-of-freedom (dof) electromechanical model of a structure with piezoelectric elements coupled to SSDS and SSDI electric circuits have been derived. By restricting the analysis to one mechanical dof only, the system free response has been analytically obtained. A similar analysis has been conducted to obtain the forced response of the structure subjected to a harmonic forcing of any frequency. Table 1 summarizes a few results, recalled in the following.

In the case of a free response, analytical formulas have been obtained in both cases of SSDS and SSDI. A major result is that the total damping factor of the system with a SSD device is very close to the structural damping factor ξ_r *plus* an added damping factor ξ_{add}, that depends *only on the coupling coefficient k_r of the involved mode*. We recall here that k_r is very close to the traditional effective coupling coefficient $k_r \simeq k_{\text{eff}}$. For a structure with a coupling coefficient $k_r = 0.2$ and a structural damping factor $\xi_r = 0.1\%$, one obtains 2.5% of added damping with SSDS and 10% with SSDI.

In the case of a forced response, similar results have been obtained, except that no analytical expressions are available. In both cases of SSDI and SSDS, it has been found that the system stabilizes in a periodic steady state of same frequency than the one of the forcing. Some unstable response have been found for low values of the electric resistance in SSDI. Frequency response curves have been plotted: they have a shape similar to classic resonance curves, with a maximum of amplitude at resonance. The attenuations, in dB, brought by the SSD device have been obtained numerically. They depend only on k_r and ξ_r. If $k_r = 0.2$ and $\xi_r = 0.1\%$ the attenuation is expected to be of 30 dB for SSDS and 46 dB for SSDI.

In the case of SSDI, an optimal value ξ_e^{opt} of the electric damping factor (linked to the electric resistance: R^{opt} is proportional to ξ_e^{opt}) has been found (an analytical expression has been obtained for the free response whereas only numerical plots are available for the forced response). Again, in both cases, ξ_e^{opt} depends on k_r only. However, the two values differ of a factor 2 between the free and forced vibration cases (compare Fig 4(right) and 12(left)).

As a general conclusion, it has been proved that *the only parameter that influences the performances of the SSD devices*

is the coupling coefficient, that has to be maximized in order to enhance the vibration attenuation. Then, for any value of k_r, it is possible to find optimal values of the electric parameters of the circuit. We recall here that the resistance R in the case of SSDS and the inductance L in the case of SSDI are directly related to the electric time constant, that has to be as small as possible, much smaller than the mechanical period, to ensure an efficient switching strategy. One has to choose R and L as small as possible.

Finally, the efficiency of SSD devices is compared to classic resistive (R) and resonant (RL) shunt techniques on Fig. 13. On top of showing better performances, SSD techniques don't present the major drawback of R and RL shunt techniques that need a precise tuning of the electric parameters on the mechanical resonance frequencies.

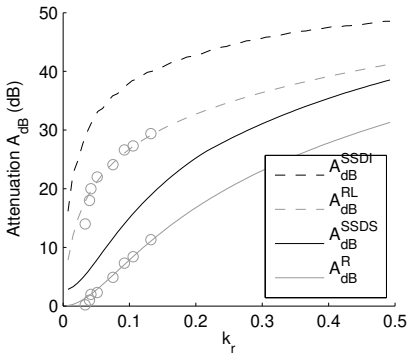

Figure 13. Expected attenuation A_{dB} as a function of coupling coefficient $k_r \simeq k_{\text{eff}}$ for SSDI, SSDS, and simple resistive (R) and resonant (RL) shunts, for $\xi_r = 0.17\%$. '—-', '– –': theory; 'o': experiments (Results on R and RL shunt from [2])

The present study can be extended to time evolution simulations of the same system with N dof, using the N dof electromechanical model of section 2. It will be possible to characterize the energy exchanges between modes and to verify if the one dof optimization described in the present study remains relevant in those more realistic cases.

ACKNOWLEDGMENT

This research is carried out under DGA contract number 05.43.063.00 470 7565 (INSA Lyon/LGEF, CNAM/LMSSc, UCBL/LENAC), for which the authors are grateful. They also wish to thank Daniel Guyomar and his team of LGEF/INSA (Lyon, France) for their advices through a training of the first author in their laboratory.

REFERENCES

[1] Hagood, N. W., and Flotow, A. V., 1991. "Damping of structural vibrations with piezoelectric materials and passive electrical networks". *Journal of Sound and Vibration,* **146**(2), pp. 243–268.

[2] Ducarne, J., Thomas, O., and Deü, J.-F., 2007. "Optimisation de dispositif passif d'atténuation de vibration par shunt piézoélectrique". In Actes du 8ème colloque national en calcul de structures, Vol. 2, Hermes, pp. 519–524. In french.

[3] Richard, C., Guyomar, D., Audigier, D., and Bassaler, H., 2000. "Enhanced semi-passive damping using continuous switching of a piezoelectric device on an inductor". In Smart Structures ans Materials : Passive Damping and Isolation, SPIE, Vol. 3989, pp. 288–299.

[4] Petit, L., Lefeuvre, E., Richard, C., and Guyomar, D., 2004. "A broadband semi passive piezoelectric technique for structural damping". In Proc. of SPIE, Vol. 5386, pp. 414–425.

[5] Corr, L. R., and Clark, W. W., 2003. "A novel semi-active multimodal vibration control law for a piezoceramic actuator". *Journal of Vibration and Acoustics,* **125**, pp. 214–222.

[6] ANSI/IEEE Std 176-1987, 1988. *IEEE Standard on Piezoelectricity*. The Institute of Electrical and Electronics Engineers, Inc.